1

2

3

4

5

Histomorphometric analyses of human adipose tissues using intact, flash-frozen samples

8

Sofia Laforest[1,2,3], Mélissa Pelletier[1,2] Andréanne Michaud[4], Marleen Daris[5], Justine Descamps[6], Denis Soulet[6], Michael D Jensen[7] and André Tchernof[1,2,3]

Author affiliations:

1: Endocrinology and Nephrology, CHU de Quebec-Laval University, Quebec City, Canada;
2: Quebec Heart Lung Institute, Quebec City, Canada;
3: School of Nutrition, Laval University, Quebec City, Canada;
4: Neurological Institute, McGill University, Montreal, Canada;
5: Gynecology Unit, Laval University Medical Center, Quebec City, Canada;
6: CHU de Québec Research Center, Neurosciences, Quebec City, Quebec, Canada; Faculty of Pharmacy, Laval University, Quebec City, Quebec, Canada; Faculty of Medicine.
7: Endocrine Research Unit, Mayo Clinic, Rochester, MN, USA.

Running Title: Cell sizing of intact, flash-frozen adipose tissue
Word count of text: 2994
Word count of abstract: 216
References: 25
Figures and Tables: 10

***Address for correspondenc*e:**   André Tchernof, Ph.D.
                Endocrinology and Nephrology
                CHU de Quebec-Laval University
                2705 Laurier Blvd. (R-4779)
                Québec, (Québec)
                CANADA   G1V 4G2
                Tel: (418) 654-2296
                Fax: (418) 654-2761
                E-mail: andre.tchernof@crchudequebec.ulaval.ca

Keywords: adipocyte hypertrophy, immunohistochemistry, image analysis, macrophages, frozen tissue

46   **Abstract**

47   Histomorphometric analyses of adipose tissue usually require formalin fixation of fresh

48   samples. Our objective was to determine if intact, flash-frozen whole adipose tissue

49   samples stored at -80°C could be used for measurements developed for fresh-fixed

50   adipose tissues. Portions of adipose tissue samples were either formalin-fixed

51   immediately upon sampling or flash-frozen and stored at -80°C and then formalin-fixed

52   during the thawing process. Mean adipocyte diameter was measured.

53   Immunohistochemistry was performed on additional samples to identify macrophage

54   subtypes (M1, CD14+ and M2, CD206+) and total (CD68+) number. All slides were

55   counterstained using haematoxylin & eosin (H&E). Visual inspection of H&E-stained

56   adipose tissue slides performed in a blinded fashion showed little or no sign of cell

57   breakage in 74% of frozen-fixed samples and in 68% of fresh-fixed samples (p>0.5).

58   There was no difference in the distribution frequencies of adipocyte sizes in fresh-fixed

59   vs. frozen-fixed tissues in both depots (p>0.9). Mean adipocyte size from frozen-fixed

60   samples correlated significantly and positively with adipocyte size from fresh-fixed

61   samples (r=0.74, p<0.0001, for both depots). The quality of staining/immunostaining and

62   appearance of tissue architecture were comparable in fresh-fixed vs. frozen-fixed

63   samples. In conclusion, intact flash-frozen adipose tissue samples stored at -80°C can be

64   used to perform techniques conventionally applied to fresh-fixed samples. This approach

65   will allow retrospective studies with frozen human adipose tissue samples.

Introduction

67   Adipose tissue expansion occurs through increases in the volume of adipocytes

68   (adipocyte hypertrophy) and/or increases in the total number of adipocytes (Cristancho

69   and Lazar 2011; Lowe et al. 2011). Hypertrophy of mature adipocytes is linked to altered

70   adipose tissue function, a phenomenon that is independent of concomitant differences in

71   total adiposity (Arner et al. 2010; Bjorntorp et al. 1971; Hoffstedt et al. 2010; Ledoux et

72   al. 2010; Lundgren et al. 2007; Veilleux et al. 2011; Weyer et al. 2000). The

73   accumulation of visceral fat is also a strong predictor of the metabolic complications

74   associated with obesity (reviewed in (Tchernof and Després 2013)). Expansion of

75   visceral adipose tissue is thought to be related to limited expandability of subcutaneous

76   fat, which limits the storage of excess dietary fatty acids (Tchernof and Després 2013).

77   Adipocyte size represents a major marker of the metabolic profile of obese patients and

78   varies according to the metabolic status of their various fat compartments (Laforest et al.

79   2015; Laforest et al. 2017). We have previously shown that adipocyte size can be

80   assessed through three techniques currently utilized in the literature and these methods

81   generate similar associations with adiposity and metabolic variables (Laforest et al.

82   2017). However, only histological analysis can be used to study tissue architecture

83   (Laforest et al. 2017). Adipocyte hypertrophy is associated with increased macrophage

84   infiltration in adipose tissue, thus contributing to the local and systemic inflammation

85   observed in obesity and insulin resistance (Michaud et al. 2012; Michaud et al. 2013).

86   Using histomorphometric analyses of adipose tissue, we have shown that pericellular

87   fibrosis in adipose tissue, but not total fibrosis, is associated with a detrimental metabolic

88   profile (Michaud et al. 2016), thus enhancing the importance of studying *in situ* markers

89 of adipose tissue dysfunction to better understand the physiopathology of obesity and

90 concomitant diseases such as type 2 diabetes.

91

92 According to available literature, no attempt has been made to measure the size of

93 adipocytes after flash freezing, regardless of the use and type of cryoprotective agents

94 (Son et al. 2010; Wolter et al. 2005). Because adipocytes contain less water than most

95 cell types, there is a reduced possibility of ice crystals formation, the main cause of cell

96 membrane breakage during the thawing process. Our working hypothesis was that it is

97 feasible to preserve the integrity of tissue architecture and consequently quantify cell size

98 in tissue that was frozen in liquid nitrogen and stored at -80°C without cryoprotectant.

99 We also postulated that immunohistochemistry (IHC) characterization of the infiltrating

100 macrophages is also possible in these samples. We tested the hypothesis that cell size

101 measurements and macrophage quantification in frozen and subsequently fixed adipose

102 tissue samples is comparable to measurements obtained in portions of the same samples

103 that were fixed in the fresh state. The usefulness of frozen adipose tissue in

104 histomorphometric analysis is of the utmost importance in the field of obesity and would

105 allow for retrospective studies in large tissue banks.

106 **Materials and Methods**

107 *Participant recruitment*

108 Women undergoing gynecological surgery were enrolled at the Gynecology Unit of CHU

109 de Quebec-Laval University Medical Center. The study was approved by the Research

110 Ethics Committees of Laval University Medical Center (C09-08-086). Samples were also

111   obtained from research volunteers participating in IRB-approved studies of obesity at

112   Mayo Clinic. All procedures performed were in agreement with the ethical guidelines of

113   the Declaration of Helsinki and its later amendments. All subjects provided written

114   informed consent before their inclusion in the study.

115   *Adipose tissue samples*

116   Subcutaneous (SC) (n=29) and omental (OM) (n=29) adipose tissue samples were

117   collected during the surgical procedure at the site of incision (lower abdomen) and at the

118   distal portion of the greater omentum, respectively at the CHU de Quebec-Laval

119   University Medical Center. At Mayo Clinic, SC adipose tissue from abdomen (n=4) for

120   direct comparison of freshly fixed vs. frozen-fixed tissue and an additional set of samples

121   (n=6) and thigh (n=7) were collected for frozen-fixed analysis. All biopsies were

122   performed under local anesthesia using sterile technique. Samples were

123   immediately carried to the laboratory. To measure adipocyte size, a portion of the sample

124   was fixed in 10% buffered formalin for 24 to 48 hours at room temperature and then

125   processed for standard paraffin embedding. The remaining portion of the sample was

126   immediately flash frozen with liquid nitrogen and subsequently kept at -80°C.

127   *Fixation of frozen adipose tissue*

128   A container was filled with dry ice to keep surgical instruments cold (tweezers, scalpel

129   and scissors). Precautions were also taken so that frozen adipose tissue samples never

130   thawed during weighing and preparation. Surgical instruments were used to collect a

131   subsample of 50-100 mg from frozen tissue pieces kept on dry ice. The subsamples were

132   then transferred to a 5 mL tube kept cold and immediately stored in a -80°C freezer until

133   fixation. The frozen tissue pieces were then fixed in 10% buffered formalin kept at 4°C

134   for 24 to 48 hours. No thawing of the adipose tissue samples was performed prior to

135   incubation in cold buffered formalin. Samples for IHC underwent the same processing,

136   but paraffin incubation time was limited to 24 hours to limit cross-linking of proteins

137   which may affect the quality of IHC.

138   *Cell sizing*

139   All adipose tissue slides (tissue slice thickness: 5 µm) were stained with haematoxylin &

140   eosin (H&E) for adipocyte diameter measurements. The histological H&E were

141   photographed with the help of a QImaging Retiga 2000R FAST camera (QImaging,

142   Surrey, C.B., Canada) coupled to a BX51 microscope (Olympus, Shinjuku, Tokyo,

143   Japan). Cell areas were measured with ImageJ software (according to (Parlee et al. 2014))

144   with slight modifications to the protocol (**Figure 1**). Briefly, analyses were performed in

145   a blinded fashion, without knowledge of the original patient, the type of depot (OM or

146   SC) and condition (frozen or fresh). Visual inspection of H&E-stained adipose tissue

147   slides was performed prior to cell sizing to assess the quality and quantity of the tissue.

148   For each folder of pictures, one image was randomly selected and was converted to 8-bit.

149   The background was subtracted and background noise was eliminated. A threshold was

150   set for the binary conversion, with values that were different from a group pictures to

151   another depending on the specifics of the tissue and due to uneven H&E staining. This

152   value was noted for programming of automated image analysis.

153   Pictures were treated with the steps described above in an automated manner according to

154   their threshold value. They were converted into binary, contours of the cells were dilated

155   and each cell was selected with the Wand tool, measured and labeled with the extension

156   module 'Measure and Label' of ImageJ. To prevent bias, all image files were placed in a

157   computer-generated random order. Cells had to show complete membranes to be

158   measured. The results were then converted in diameter assuming a circular surface of

159   adipocytes measured according to the following formula: $D = 2\sqrt{(A/\pi)}$. The average of

160   100 cells was used when possible.

161   ***Automated high-performance histological analysis of serial adipose tissue sections***

162   Additional SC (n=1) and OM (n=1) adipose tissue samples were collected during the

163   surgical procedure at the site of incision and greater omentum, respectively. Consent was

164   obtained through the management framework of the Quebec Heart Lung Institute Obesity

165   Tissue Bank. Samples were processed as described in *Adipose tissue samples* and the

166   *Fixation of frozen adipose tissue* sections above. Thirty consecutive 5 µm-thick sections

167   for each paraffin block (OM and SC fresh- and frozen-fixed) were cut, covering 150 µm

168   of thickness per block and stained with H&E.

169   Subsequently, slides were scanned using a Zeiss AxioScan.Z1 whole slide scanner

170   equipped with a 20X plan apochromat objective lens (NA 0.8). Since tissues stained with

171   H&E are typically autofluorescent in the red channel, the image acquisition (Zen 2.3

172   acquisition software) was performed using an AlexaFluor 555 filter set to generate

173   grayscale images. Mosaic of images were exported as BigTiff files and processed using a

174   modified algorithm used for the morphological analysis of lung alveoli as published

175   previously (Sallon et al. 2015). Briefly, Matlab software version 2014a (Mathworks) was

176   used to perform a distributed computing analysis of the images, and results were exported

177   as CSV files. Grayscale images contrast was adjusted, then images were segmented using

178   a specific threshold to generate binarized images. Closed structures were identified and

179   sorted based on their area (>1200 µm^2) and solidity values (>0.9). Thus, an adipocyte

180   with a solidity value close to 1 will be very round and smooth, while adipocytes with low

181   solidity value will be distorted or broken, hence excluded from our analysis. The

182   frequency distribution of adipocyte area was calculated using Prism 7 and distribution

183   plots were generated.

184   ***Immunohistochemistry***

185   All samples were paraffin-embedded and 5 µm sections were placed onto slides and

186   stained at the Pathology Research Core at Mayo Clinic, Rochester, MN. Each sample was

187   stained with a total macrophage and monocyte marker antibody against CD68; an M1

188   macrophage or pro-inflammatory macrophage marker antibody against CD14 and an M2

189   macrophage or anti-inflammatory macrophage marker antibody against CD206. The IHC

190   staining procedure was performed on-line using the Leica Bond III Stainer (Leica,

191   Buffalo, IL). The tissue slides were dewaxed using Bond Dewax (Leica, Buffalo, IL).

192   Tissue slides for CD14 and CD68 stain were retrieved for 20 minutes using Epitope

193   Retrieval 2 (Leica, Buffalo, IL) and slides for CD206 stain were retrieved for 20 minutes

194   using Epitope Retrieval 1 (Leica, Buffalo, IL). All primary antibodies were diluted in

195   Bond Antibody Diluent (Leica, Buffalo, IL). The primary antibody CD14 (Sigma-

196   Aldrich, St. Louis, MO) was used at 1:300; CD68 (Clone PG-M1, Dako, Carpinteria,

197   CA) was used at 1:200; and CD206 (Clone 685645, R&D Systems, Minneapolis, MN)

198   was used at 1:200. The detection system used was the Polymer Refine Detection System

199   (Leica, Buffalo, IL). This system includes the hydrogen peroxidase block, secondary

200   antibody polymer, DAB and hematoxylin. Immunostaining visualization was achieved by

201   incubating slides 10 minutes in DAB and DAB buffer (1:19 mixture) from the Bond

202   Polymer Refine Detection System. To this point, slides were rinsed between steps with 1´

203   Bond Wash Buffer (Leica, Buffalo, IL). Before and after DAB incubation, slides were

204   rinsed in distilled water. Slides were counterstained for 5 minutes using Schmidt

205   hematoxylin and molecular biology grade water (1:1 mixture), followed by several rinses

206   in 1′ Bond wash buffer and distilled water; this is not the hematoxylin provided with the

207   kit. Following completion of the IHC, processed slides were removed from the stainer

208   and rinsed in tap water for 5 minutes. Slides were dehydrated in increasing concentrations

209   of ethyl alcohol and cleared in 3 changes of xylene prior to placing a permanent coverslip

210   in xylene-based medium.

211   The stained tissue sections were then visualized by light microscopy using an Olympus

212   BX43 microscope. Ten images per slide were obtained by randomly selecting fields at

213   40x magnification. Two independent observers counted positively stained macrophages

214   and total adipocytes for each field of view. Data are expressed as mean (standard

215   deviation) number of positive cells per 100 adipocytes.

216   All slides were marked with a code rather than the source of the sample to ascertain that

217   the independent observers were blinded to the other reader's data, to the participant, the

218   research protocol, and biopsy site.

219   ***Statistical analyses***

220   Differences between positive cells/mean cell diameter in fresh- vs. frozen-fixed were

221   assessed by paired t-test. Cell size frequency distributions were assessed by the

222   Kolmogorov-Smirnov test. Pearson correlations were computed with normally distributed

223   variables according to the Shapiro-Wilk test. Distribution correction was performed

224   according to Lenz et al. (2016). This correction considers the cut-off parameter of the

225   imaging software, the use of cross-sectional images instead of 3D samples and the tissue

226   thickness. The normal distribution algorithm was used but the gamma distribution

227   algorithm generated similar results (Lenz et al. 2016). A chi-squared test was used to

228   assess differences in the proportion of damaged and/or unusable samples between the

229   fresh- and frozen-fixed methods. A p-value $\leq$ 0.05 was considered significant. All

230   statistical analyses were performed with JMP and/or SAS software (SAS Institute, Cary,

231   NC, USA).

232   **Results**

233   *Visual inspection*

234   Histological examination of fresh-fixed and frozen-fixed tissues was performed in all

235   samples to determine whether intact, flash-frozen adipose tissue showed signs of cell

236   breakage and alteration of the architecture of adipose tissue after thawing and fixation.

237   **Figure 2** shows representative pictures of frozen- and fresh-fixed adipose tissue. Slightly

238   more apparent tissue shrinkage, damage and other alterations were observed in the fresh

239   samples. However, the proportion of unusable samples was not different in the frozen-

240   fixed vs. fresh-fixed methods (p=0.54). Samples with large amounts of stromal tissue

241   (capillaries, fibroblasts, etc.) appeared to show more damage.

242   As the morphology of the tissue was retained in most samples, both fresh- and frozen-

243   fixed, we performed IHC to label macrophages. Macrophage detection is one of the most

244   used procedure performed on fresh-fixed fat samples to further characterize the tissue.

245   Preliminary tests showed that the antibodies still retain the ability to bind corresponding

246   cell surface markers in frozen adipose tissue (**Figure 3**).

247 *Immunohistochemistry*

248 We compared 4 slides that had been frozen and then fixed with slides from the same

249 freshly fixed tissue for CD68, CD14 and CD206 stained macrophages. Freshly fixed

250 tissue had 27(16), 8(6), and 22(10), CD68, CD14 and CD206 macrophages/100

251 adipocytes, respectively. For the frozen-fixed tissue these values were 18(15), 7(4), and

252 20(4), CD68, CD14 and CD206 macrophages per 100 adipocytes, respectively (standard

253 deviation values in parentheses). Representative images are shown in **Figure 3**, **4** and **5**,

254 for CD68, CD206 and CD14, specifically. Paired t-tests showed no difference between

255 fresh- vs. frozen-fixed for CD68-, CD206- or CD14- positive cells (**Figure 6**).

256 We used frozen tissue from an additional 7 volunteers (13 slides, 7 thigh and 6 abdomen)

257 to further test the frozen-fixation protocol. For these 13 slides, we found that there were

258 14(5), 7(2), and 13(3), CD68, CD14 and CD206 macrophages per 100 adipocytes,

259 respectively (data not shown).

260 *Adipocyte size*

261 Mean cell size distribution curves from OM and SC fresh- and frozen-fixed tissue are

262 shown in **Figure 7** and **8**. There was no difference in cell size distributions (p>0.90) and

263 in mean adipocyte sizes (**Figure 7** and **8**). Furthermore, in both OM and SC samples,

264 adipocyte mean diameters from fresh- and frozen-fixed samples were strongly

265 intercorrelated (r=0.74, p<0.0001, for both) (**Figure 7** and **8**). We also presented the same

266 analysis with the corrected cell size distributions for both depots and both conditions

267 (**Figure 7** and **8**) as proposed by Lenz and collaborators to reduce measurement bias

268 (Lenz et al. 2016). We performed automated, high-performance histological analysis of

269 30 consecutive cross-sectional adipose tissue sections covering 150 µm for both depots

270 and both conditions. Distribution of adipocyte area was not significantly different across

271 conditions for each depot (**Figure 9**). In **Figure 10**, we present cell size distributions and

272 main characteristics from two different patients to illustrate individual heterogeneity.

273 **Discussion**

274 We investigated if it was possible to evaluate adipocyte size, tissue architecture and

275 macrophage infiltration in intact, frozen whole adipose tissue stored at -80°C. We

276 demonstrated here for the first time that flash-frozen adipose tissue, without use of

277 cryoprotective agents, can be utilized to assess fat cell size mean diameter and

278 distribution. Furthermore, antigen labeling can be performed in a similar fashion, as

279 shown by macrophage detection by IHC. These results are consistent with those reported

280 in fresh-fixed adipose tissue in our study. We acknowledge the inherent limitations

281 related to histological assessment of adipocyte cell size (Laforest et al. 2017). Our

282 attempts to apply stereological principles to cell sizing analyses in the present study were

283 unsuccessful. Our assessment is that the very large size of human adipocytes, especially

284 in obese individuals, makes the use of stereological analysis extremely difficult. It

285 requires registering pairs of very large images, and overlaying unbiased stereological

286 frames over precisely matching regions in both the reference and look-up sections is not

287 possible, or introduces bias in the quantification.

288 The main strength of our study is that we were able to perform this experiment and

289 validate its use in two different research centers. Moreover, all independent observers

290 were blinded to other reader's data, to the biopsy site, to the state of tissue (fresh-fixed or

291 frozen-fixed), to the research protocol and to the participant. We also added corrected

292   adipocyte diameter, as proposed by Lenz et al. (2016) and found comparable results. In

293   additional samples, we also performed an automated analysis of multiple slices covering

294   150 µm in both depots and conditions and found no difference in cell size distribution or

295   mean cell size.

296   Previous studies used fresh-fixed tissue for obvious and practical reasons. However, the

297   utility of frozen-fixed tissue sections of adipose tissue may be of great importance for

298   researchers in the field of obesity (Ashwell et al. 1975). Some large cohorts may have

299   only flash-frozen adipose tissue due to various rationales (cell size assessed by

300   collagenase or by osmium instead of histological analysis, tissues kept only for RNA or

301   DNA analyses, etc.) and are possibly lacking important *in situ* characterization. This

302   novel method offers a unique opportunity to study markers of adipose tissue function or

303   dysfunction in samples that could not be studied before. Investigators have used frozen

304   adipose tissue in previous publications. However, it was always fixed prior to the

305   freezing (Berry et al. 2014; Sjostrom et al. 1971) or placed in OCT compounds (Xue et

306   al. 2010). Yuan and collaborators have published an interesting hypothesis in which they

307   suggested that freezing adipose tissue at -20°C without cryoprotectant and thawing it at

308   room temperature (3 days later) affected cell viability and caused necrosis of the tissue

309   without damaging whole tissue architecture (Yuan et al. 2015). Our results suggest that it

310   is in fact possible to observe and characterize *in situ* markers of adipose tissue in flash-

311   frozen samples stored for at least three years at -80°C.

312   We anticipate that this approach will allow retrospective studies with flash-frozen human

313   adipose tissue samples and will shed some light on the importance of adipose tissue in the

314   pathogenesis of obesity, especially excess abdominal adiposity.

315 **Conflict of interest**

316 AT is the recipient of research grant support from Johnson & Johnson Medical

317 Companies for studies unrelated to this publication. No author declared a conflict to

318 interest.

319 **References**

320 Arner E et al. (2010) Adipocyte turnover: relevance to human adipose tissue morphology.
321   Diabetes 59:105-109 doi:10.2337/db09-0942

322 Ashwell MA, Priest P, Sowter C (1975) Importance of fixed sections in the study of
323   adipose tissue cellularity. Nature 256:724-725

324 Berry R, Church CD, Gericke MT, Jeffery E, Colman L, Rodeheffer MS (2014) Imaging
325   of adipose tissue. Methods Enzymol 537:47-73 doi:10.1016/b978-0-12-411619-
326   1.00004-5

327 Björntorp P et al. (1971) Adipose tissue fat cell size and number in relation to metabolism
328   in randomly selected middle-aged men and women. Metabolism 20:927-935

329 Cristancho AG, Lazar MA (2011) Forming functional fat: a growing understanding of
330   adipocyte   differentiation.   Nat   Rev   Mol   Cell   Biol   12:722-734
331   doi:10.1038/nrm3198

332 Hoffstedt J et al. (2010) Regional impact of adipose tissue morphology on the metabolic
333   profile in morbid obesity. Diabetologia 53:2496-2503 doi:10.1007/s00125-010-
334   1889-3

335 Laforest S, Labrecque J, Michaud A, Cianflone K, Tchernof A (2015) Adipocyte size as a
336   determinant of metabolic disease and adipose tissue dysfunction. Crit Rev Clin
337   Lab Sci 52:301-313 doi:10.3109/10408363.2015.1041582

338 Laforest S, Michaud A, Paris G, Pelletier M, Vidal H, Geloën A, Tchernof A (2017)
339   Comparative analysis of three human adipocyte size measurement methods and
340   their   relevance   for   cardiometabolic   risk.   Obesity   25:122-135
341   doi:10.1002/oby.21697

342 Ledoux S et al. (2010) Traditional anthropometric parameters still predict metabolic
343   disorders   in   women   with   severe   obesity.   Obesity   18:1026-1032
344   doi:10.1038/oby.2009.349

345 Lenz M et al. (2016) Estimating real cell size distribution from cross-section microscopy
346   imaging. Bioinformatics 32:i396-i404 doi:10.1093/bioinformatics/btw431

347 Lowe CE, O'Rahilly S, Rochford JJ (2011) Adipogenesis at a glance. J Cell Sci
348   124:2681-2686 doi:10.1242/jcs.079699

349 Lundgren M, Svensson M, Lindmark S, Renstrom F, Ruge T, Eriksson JW (2007) Fat
350   cell enlargement is an independent marker of insulin resistance and
351   'hyperleptinaemia'. Diabetologia 50:625-633 doi:10.1007/s00125-006-0572-1

352 Michaud A, Drolet R, Noël S, Paris G, Tchernof A (2012) Visceral fat accumulation is an
353   indicator of adipose tissue macrophage infiltration in women. Metabolism 61:689-
354   698 doi:10.1016/j.metabol.2011.10.004

355 Michaud A, Pelletier M, Noël S, Bouchard C, Tchernof A (2013) Markers of macrophage
356   infiltration and measures of lipolysis in human abdominal adipose tissues. Obesity
357   21:2342-2349 doi:10.1002/oby.20341

358 Michaud A et al. (2016) Relevance of omental pericellular adipose tissue collagen in the
359   pathophysiology of human abdominal obesity and related cardiometabolic risk.
360   Int J Obes 40:1823-1831 doi:10.1038/ijo.2016.173

361 Parlee SD, Lentz SI, Mori H, MacDougald OA (2014) Quantifying size and number of
362   adipocytes in adipose tissue. Methods Enzymol 537:93-122 doi:10.1016/b978-0-
363   12-411619-1.00006-9

364 Sallon C, Soulet D, Provost PR, Tremblay Y (2015) Automated High-Performance
365   Analysis of Lung Morphometry. Am J Respir Cell Mol Biol 53:149-58 doi:
366   10.1165/rcmb.2014-0469MA

367 Sjöström L, Björntorp P, Vrana J (1971) Microscopic fat cell size measurements on
368   frozen-cut adipose tissue in comparison. J Lipid Res 12:521-530

369 Son D, Oh J, Choi T, Kim J, Han K, Ha S, Lee K (2010) Viability of fat cells over time
370   after syringe suction lipectomy: the effects of cryopreservation. Ann Plast Surg
371   65:354-360 doi:10.1097/SAP.0b013e3181bb49b8

372 Tchernof A, Després JP (2013) Pathophysiology of human visceral obesity: an update.
373   Physiol Rev 93:359-404 doi:10.1152/physrev.00033.2011

374 Veilleux A, Caron-Jobin M, Noël S, Laberge PY, Tchernof A (2011) Visceral adipocyte
375   hypertrophy is associated with dyslipidemia independent of body composition and
376   fat distribution in women. Diabetes 60:1504-1511 doi:10.2337/db10-1039

377 Weyer C, Foley JE, Bogardus C, Tataranni PA, Pratley RE (2000) Enlarged subcutaneous
378   abdominal adipocyte size, but not obesity itself, predicts type II diabetes
379   independent of insulin resistance. Diabetologia 43:1498-1506
380   doi:10.1007/s001250051560

381 Wolter TP, von Heimburg D, Stoffels I, Groeger A, Pallua N (2005) Cryopreservation of
382   mature human adipocytes: in vitro measurement of viability. Ann Plast Surg
383   55:408-413

384 Xue Y, Lim S, Brakenhielm E, Cao Y (2010) Adipose angiogenesis: quantitative
385   methods to study microvessel growth, regression and remodeling in vivo. Nat
386   Protoc 5:912-920 doi:10.1038/nprot.2010.46

387 Yuan Y, Chen C, Zhang S, Gao J, Lu F (2015) The role of the intact structure of adipose
388   tissue in free fat transplantation. Exp Dermatol 24:238-239
389   doi:10.1111/exd.12631

390   **Fig. 1** Image processing for adipocyte size measurements

391   **Fig. 2** Representative images of frozen-fixed and fresh-fixed adipose tissue. (a) Frozen-
392   fixed and (b) Fresh-fixed sample from the same woman showing little or no sign of cell
393   breakage (representative of 74% and 68% of samples, respectively). (c) Frozen-fixed and
394   (d) Fresh-fixed sample from the same woman showing (arrows) signs of cell breakage
395   (representative of 26% and 32% of samples, respectively). Scale bars from complete scan
396   represented 500 µm and from zoom image, Scale bars 50 µm

397   **Fig. 3** Representative images of fresh-fixed (a, b) and frozen-fixed (c, d) adipose tissue
398   showing CD68+ cell labeling (IHC) Scale bar: 50 µm

399   **Fig. 4** Representative images of frozen-fixed adipose tissue showing CD206+ cell
400   labeling (IHC) Scale bar: 50 µm

401   **Fig. 5** Representative images of frozen-fixed adipose tissue showing CD14+ cell labeling
402   (IHC) Scale bar: 50 µm

403   **Fig. 6** Number of CD68-, CD206- or CD14-positive cells per 100 adipocytes in fresh- vs.
404   frozen-fixed adipose tissue as measured by IHC

405   **Fig. 7** Adipocyte size frequency distribution from (a) OM fresh-fixed and frozen-fixed
406   adipose tissue samples (n=17) and (d) corrected OM, showing similar profiles (p>0.05).
407   Correlation between adipocyte mean diameter in fresh- vs. frozen-fixed (b) OM (r=0.72;
408   p<0.01) and (e) corrected OM (r=0.73; p<0.001). No significant difference between
409   adipocyte mean diameter in (c) OM fresh- vs. frozen-fixed (Student paired t-test; p>0.05)
410   and (f) corrected OM (Student paired t-test; p>0.05). These analyses were performed in a
411   subset of patients with at least 20 adipocytes per depot measured

412   **Fig. 8** Adipocyte size frequency distribution from (a) SC fresh-fixed and frozen-fixed
413   adipose tissue samples (n=13) and (d) corrected SC, showing similar profiles (p>0.05).
414   Correlation between adipocyte mean diameter in fresh- vs. frozen-fixed (b) SC (r=0.81;
415   p<0.001) and (e) corrected SC (r=0.72; p<0.01). No significant difference between
416   adipocyte mean diameter in (c) SC fresh- vs. frozen-fixed (Student paired t-test; p>0.05)
417   and (f) corrected SC (Student paired t-test; p>0.05). These analyses were performed in a
418   subset of patients with at least 20 adipocytes per depot measured

419   **Fig. 9** Adipocyte area frequency distribution derived from automated, high-performance
420   histological analysis of serial adipose tissue sections covering 150 µm of both (a) OM
421   and SC fresh- and frozen-fixed tissues. (b) No significant difference in adipocyte cell size
422   frequencies in OM or SC fresh- vs. frozen-fixed was observed (Student t-test; p>0.05)

423   **Fig. 10** Adipocyte size frequency distribution from Patient A (a) OM; (b) SC; and from
424   Patient B (d) OM; (e) SC; fresh-fixed and frozen-fixed adipose tissue samples. Main
425   characteristics are shown for both patients (c, f)

426
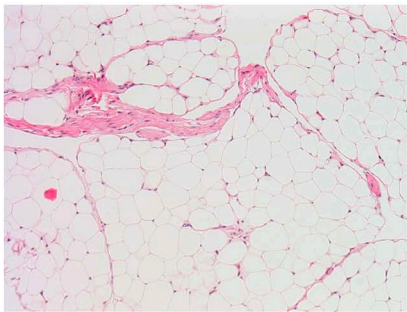
Step 1:
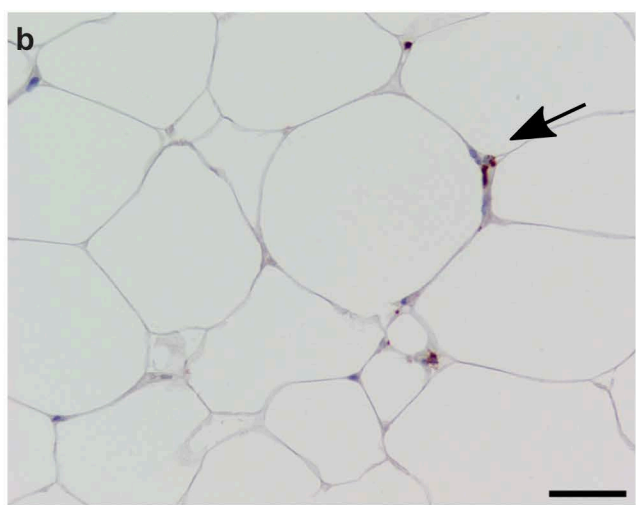Original Picture
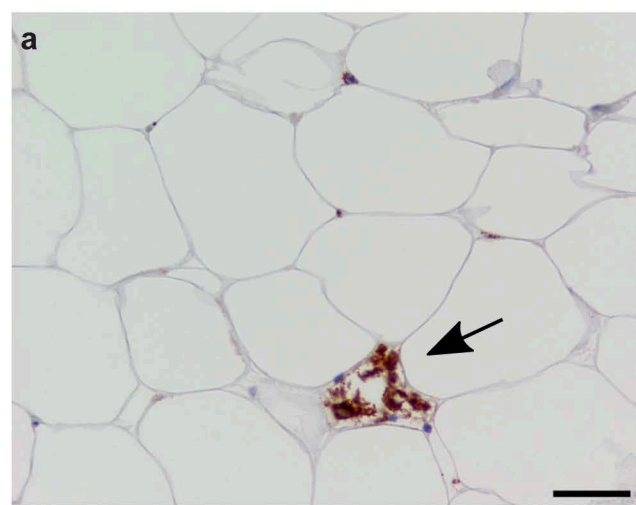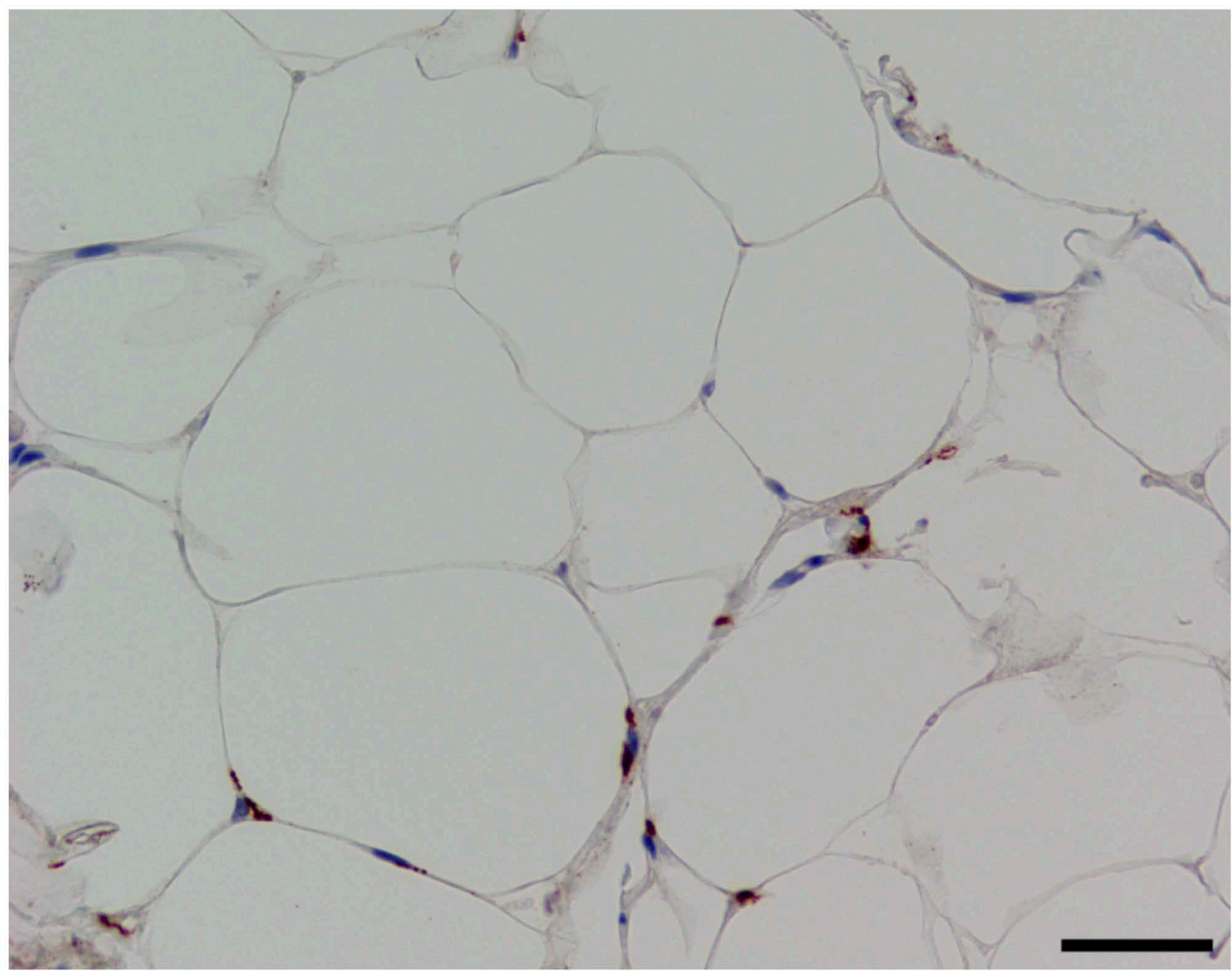(RGB-color)
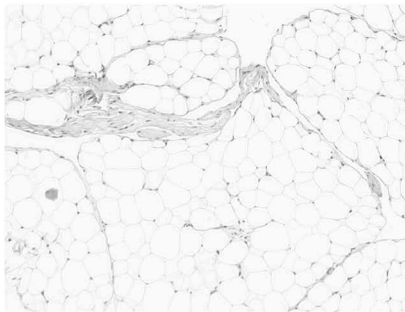
Step 2:
8-bit, Substract Background,
Despeckle
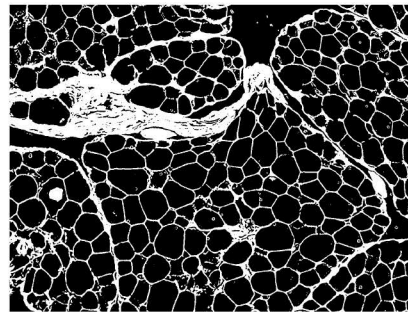
Step 3:
Threshold
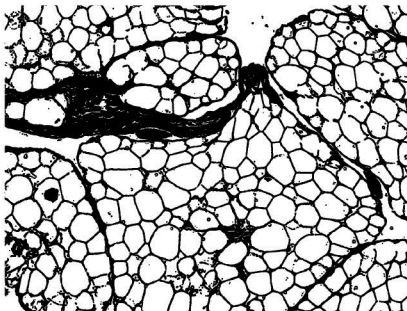
Step 4:
Make Binary, Dilate
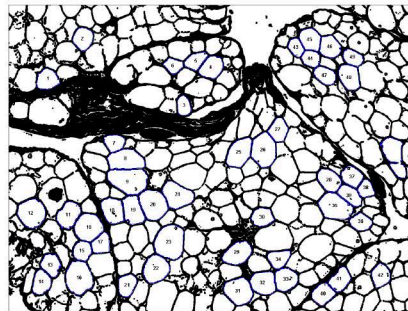
Step 5:
Quantification
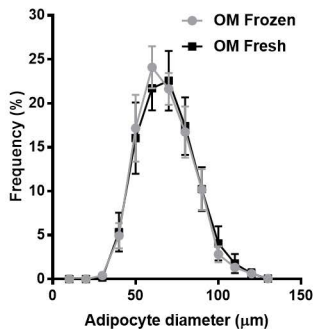
a
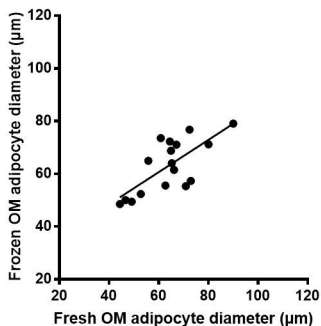

b

a

Frequency (%) vs Adipocyte diameter (μm)
OM Frozen
OM Fresh

b

Frequency (%) vs Adipocyte diameter (μm)
SC Frozen
SC Fresh

d

Frequency (%) vs Adipocyte diameter (μm)
OM Frozen
OM Fresh

e

Frequency (%) vs Adipocyte diameter (μm)
SC Frozen
SC Fresh
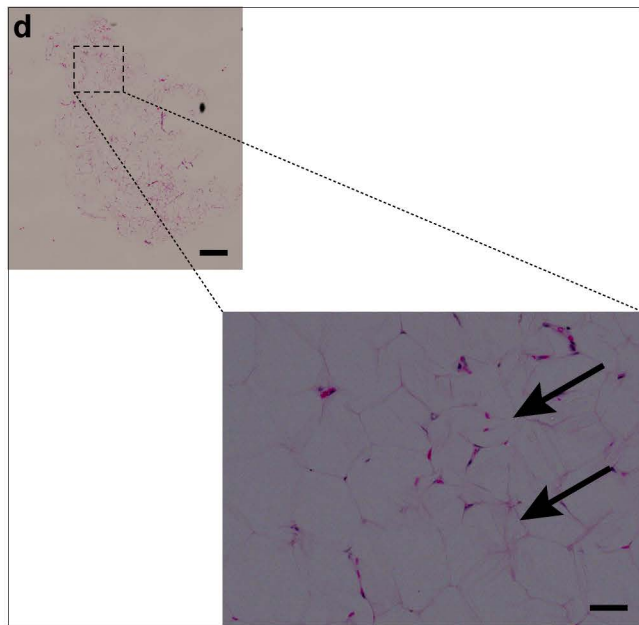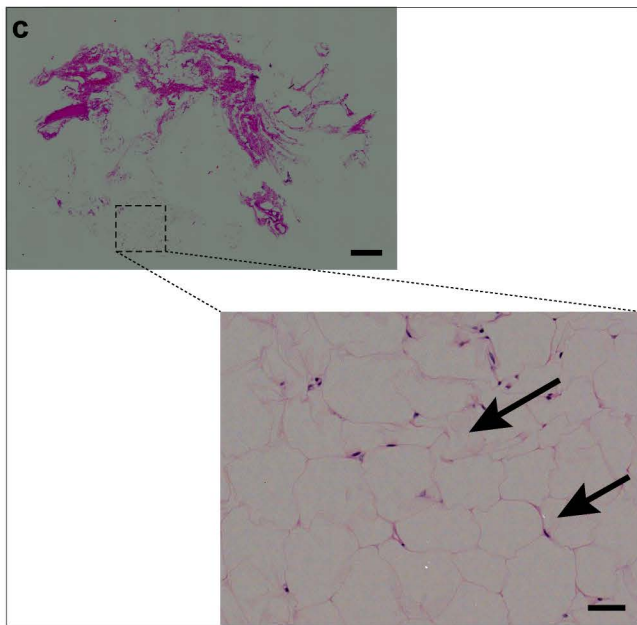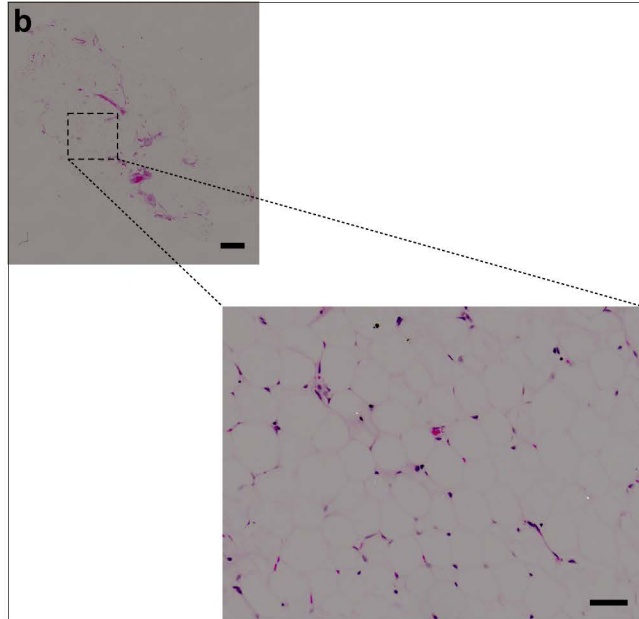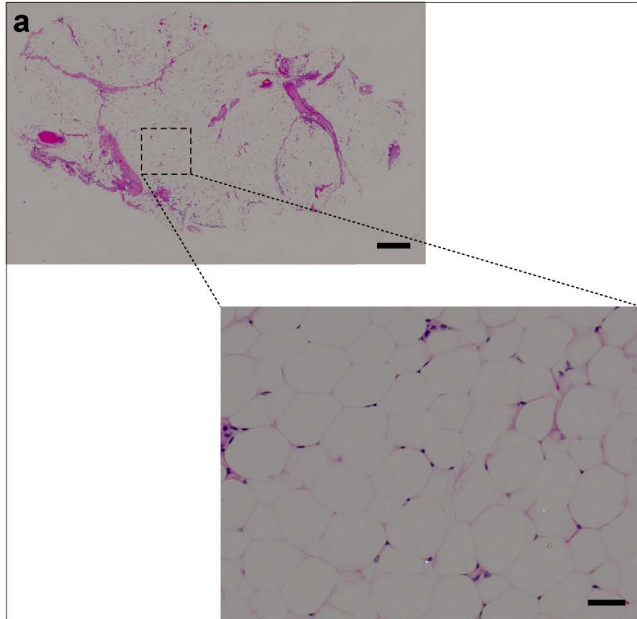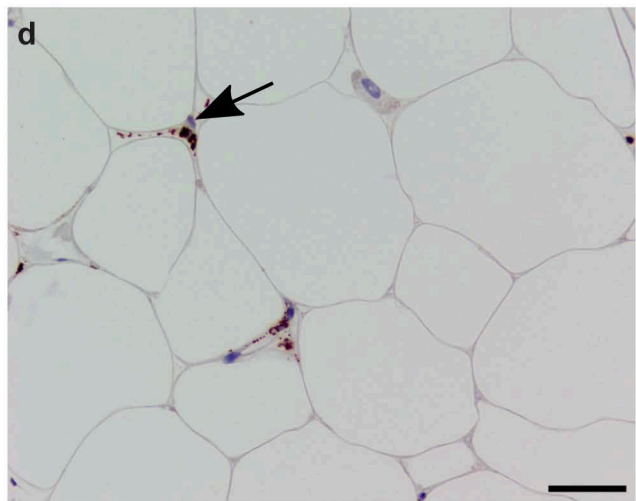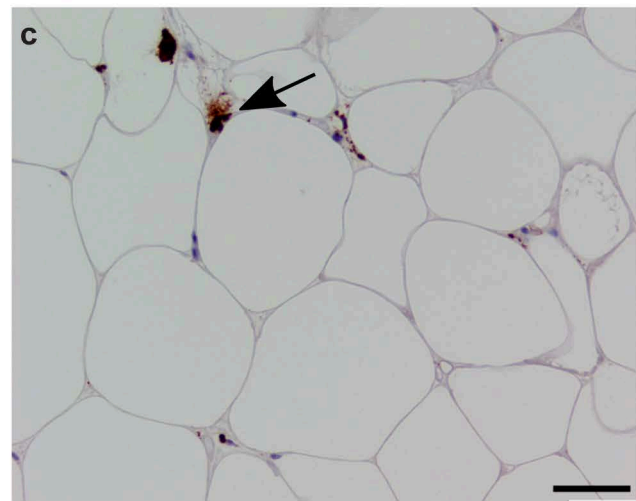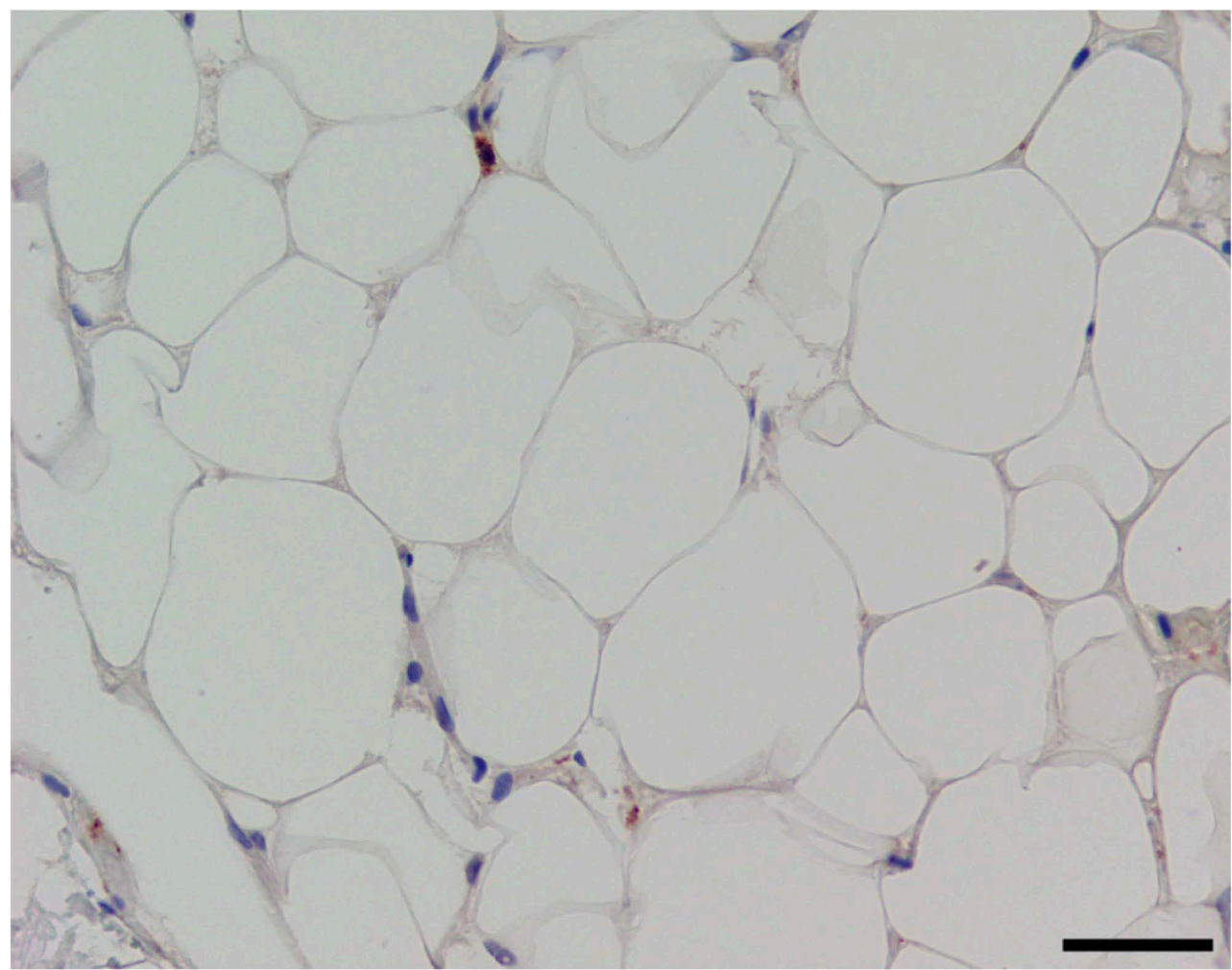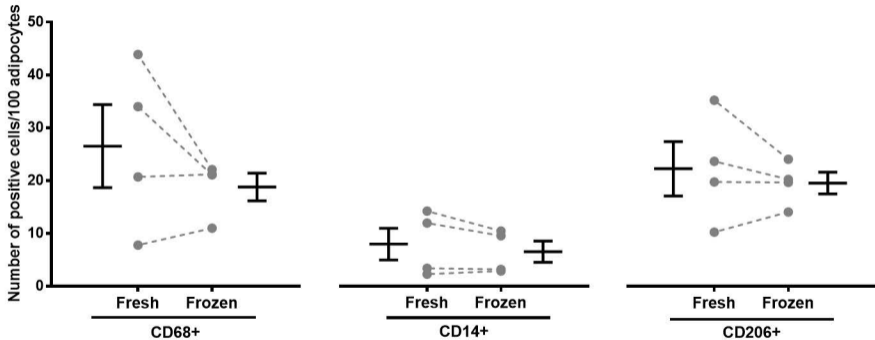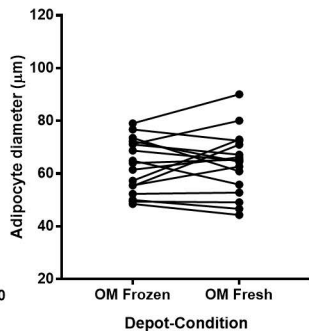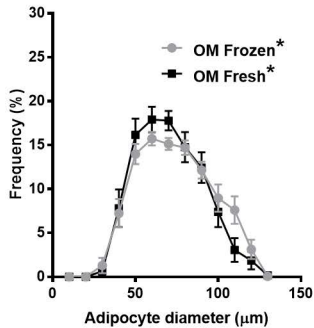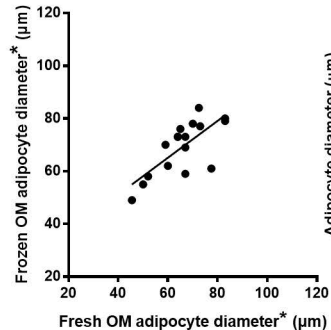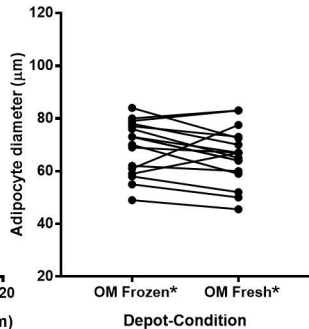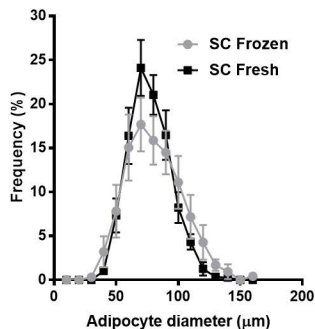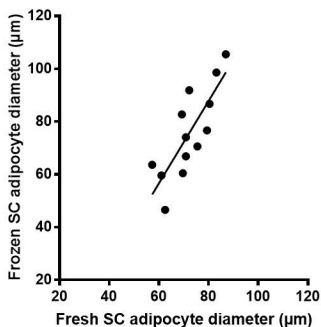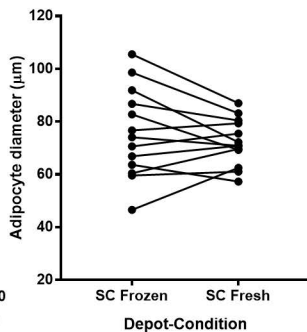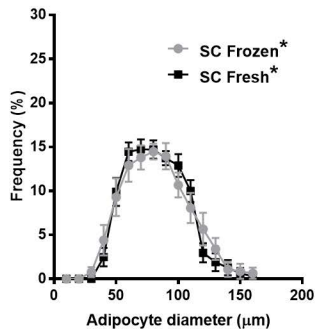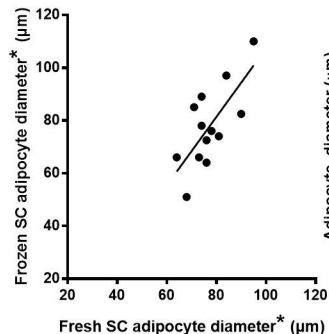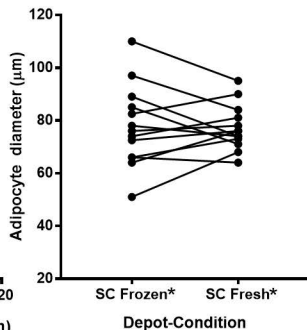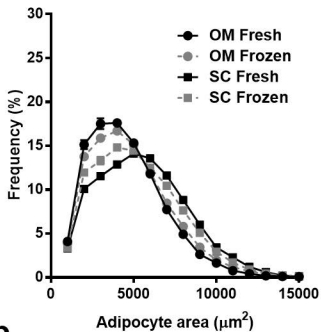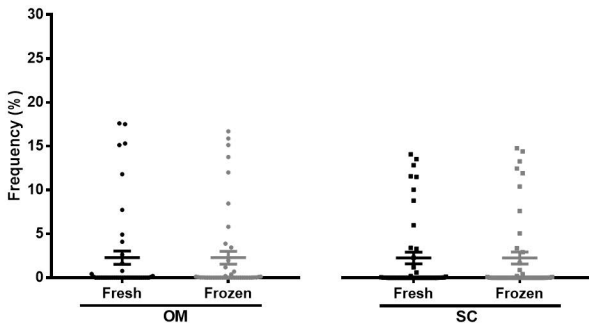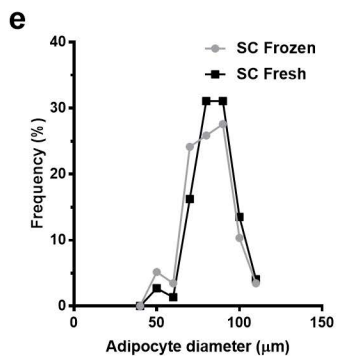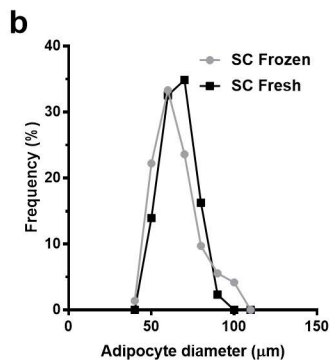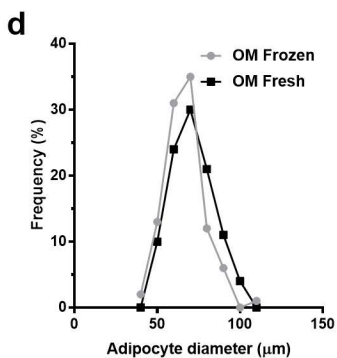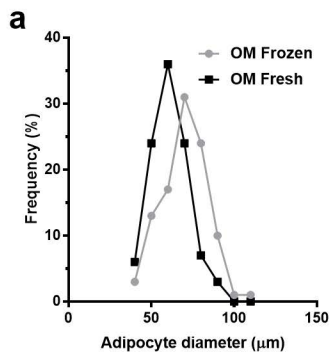
c

Patient A	
BMI (kg/m^2)	23
Age (y)	52
OM mean adipocyte diameter (μm)	56
SC mean adipocyte diameter (μm)	61

f

Patient B	
BMI (kg/m^2)	29
Age (y)	52
OM mean adipocyte diameter (μm)	66
SC mean adipocyte diameter (μm)	79